



Publication Year	2015
Acceptance in OA@INAF	2020-07-08T14:36:30Z
Title	$\beta\gamma$ Bright [C II] 158 μ m Emission in a Quasar Host Galaxy
Authors	Banados, E.; DECARLI, ROBERTO; Walter, F.; Venemans, B.P.; Farina, E.P.; et al.
DOI	10.1088/2041-8205/805/1/L8
Handle	http://hdl.handle.net/20.500.12386/26389
Journal	THE ASTROPHYSICAL JOURNAL LETTERS

BRIGHT [C II] 158 μm EMISSION IN A QUASAR HOST GALAXY AT $z = 6.54^*$ E. BAÑADOS¹, R. DECARLI¹, F. WALTER¹, B. P. VENEMANS¹, E. P. FARINA¹, AND X. FAN²¹Max Planck Institut für Astronomie, Königstuhl 17, D-69117, Heidelberg, Germany; banados@mpia.de²Steward Observatory, The University of Arizona, 933 North Cherry Avenue, Tucson, AZ 85721-0065, USA

Received 2015 April 2; accepted 2015 April 17; published 2015 May 18

ABSTRACT

The [C II] 158 μm fine-structure line is known to trace regions of active star formation and is the main coolant of the cold, neutral atomic medium. In this Letter, we report a strong detection of the [C II] line in the host galaxy of the brightest quasar known at $z > 6.5$, the Pan-STARRS1 selected quasar PSO J036.5078+03.0498 (hereafter P036+03), using the IRAM NOEMA millimeter interferometer. Its [C II] and total far-infrared luminosities are $(5.8 \pm 0.7) \times 10^9 L_\odot$ and $(7.6 \pm 1.5) \times 10^{12} L_\odot$, respectively. This results in an $L_{[\text{C II}]} / L_{\text{TIR}}$ ratio of $\sim 0.8 \times 10^{-3}$, which is at the high end of those found for active galaxies, though it is lower than the average found in typical main-sequence galaxies at $z \sim 0$. We also report a tentative additional line that we identify as a blended emission from the $3_{22} - 3_{13}$ and $5_{23} - 4_{32}$ H₂O transitions. If confirmed, this would be the most distant detection of water emission to date. P036+03 rivals the current prototypical luminous J1148+5251 quasar at $z = 6.42$, in both rest-frame UV and [C II] luminosities. Given its brightness and because it is visible from both hemispheres (unlike J1148+5251), P036+03 has the potential of becoming an important laboratory for the study of star formation and of the interstellar medium only ~ 800 Myr after the Big Bang.

Key words: cosmology: observations – quasars: emission lines – quasars: general

1. INTRODUCTION

The study of star formation in the first galaxies back in the epoch of reionization ($z > 6.5$) is one of the main challenges in current observational cosmology.

Several groups have tried to identify the [C II] 158 μm fine-structure transition line (hereafter [C II]) in the first spectroscopically identified galaxies at these redshifts. The [C II] line is the dominant coolant of interstellar neutral gas and is one of the brightest lines in the spectrum of star-forming galaxies, accounting for up to $\sim 1\%$ of the total far-infrared (FIR) luminosity in $z \sim 0$ main-sequence galaxies. Studies of the [C II] line may also provide key insights into galaxy kinematics at the highest redshifts (see Carilli & Walter 2013 for a review). However, thus far, there are no convincing detections of [C II] emission from star-forming galaxies during the epoch of reionization (Walter et al. 2012; Kanekar et al. 2013; Ouchi et al. 2013; González-López et al. 2014; Ota et al. 2014; Schaerer et al. 2015; Watson et al. 2015; but see also the recent work of Maiolino et al. 2015).

On the other hand, the [C II] line has been identified in a number of more extreme objects such as submillimeter galaxies and quasar host galaxies at $z \sim 6$ (Maiolino et al. 2005; Walter et al. 2009a; Riechers 2013; Wang et al. 2013; Willott et al. 2013, 2015). These objects are most likely the progenitors of massive early-type galaxies seen in the present universe. Thus, luminous quasars are thought to be important tools to pinpoint the locations of these extreme galaxies in the early universe. Indeed, the [C II] line has been detected even in the host galaxy of the currently most distant quasar known at $z = 7.1$ (Venemans et al. 2012).

For more than a decade, the quasar SDSS J1148+5251 at $z = 6.42$ (hereafter J1148+5251), discovered by Fan et al. (2003), has been the brightest quasar known at $z > 6$

($M_{1450} = -27.8$). As such, it is by far the best studied quasar at these redshifts, being fundamental in shaping our current understanding of the universe when it was less than 1 Gyr old. It was the first source detected in [C II] at $z > 0.1$ (Maiolino et al. 2005), and for several years it remained the only $z > 6$ quasar also detected in CO emission (Bertoldi et al. 2003b; Walter et al. 2003, 2004; Riechers et al. 2009). The [C II] line in this quasar has been studied in detail (e.g., Walter et al. 2009a; Maiolino et al. 2012). Neutral carbon [C I] has also been detected (Riechers et al. 2009), while deep limits on the [N II] line could also be placed (Walter et al. 2009).

Recently, and after more than 10 years, three quasars that rival (and in one case even surpass) J1148+5251 in UV–luminosity have been discovered. These quasars are SDSS J0100+2802 ($z = 6.30$; $M_{1450} = -29.3$; Wu et al. 2015), ATLAS J025.6821–33.4627 ($z = 6.31$; $M_{1450} = -27.8$; Carnall et al. 2015), and PSO J036.5078+03.0498 (hereafter P036+03; $z = 6.527$; $M_{1450} = -27.4$; Venemans et al. 2015).

In this Letter, we focus on P036+03, which is the brightest quasar known at $z > 6.5$ (see Figure 3 in Venemans et al. 2015). We report a bright detection of the [C II] line with the IRAM NOEMA interferometer. We also detect the underlying dust FIR continuum emission and present a tentative detection of a water transition in this quasar. As a result, P036+03 (that is also accessible from telescopes in the southern hemisphere) competes with the current archetypal high-redshift quasar J1148+5251 in both rest-frame UV and [C II] luminosities.

We employ a cosmology with $H_0 = 67.8 \text{ km s}^{-1} \text{ Mpc}^{-1}$, $\Omega_M = 0.307$, and $\Omega_\Lambda = 0.691$ (Planck Collaboration et al. 2014). This implies that for $z = 6.5412$, the proper spatial scale is $5.6 \text{ kpc arcsec}^{-1}$ and the age of the universe is 833 Myr, i.e., 6% of its present age.

2. OBSERVATIONS AND RESULTS

We use the IRAM NOEMA interferometer to observe the [C II] line in the quasar P036+03, as a director’s discretionary time proposal (ID: E14AG). The tuning frequency is

* Based on observations carried out under project number E14AG with the IRAM NOEMA Interferometer. IRAM is supported by INSU/CNRS (France), MPG (Germany), and IGN (Spain).

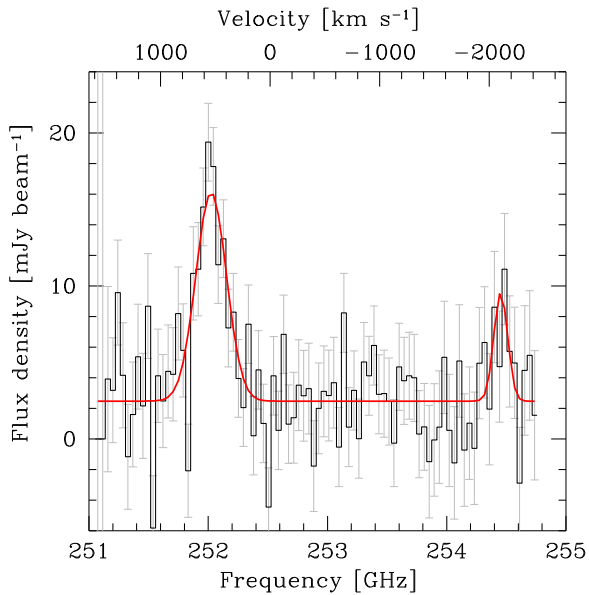


Figure 1. NOEMA spectrum at 1 mm (observed) wavelengths of P036+03. The tuning frequency was centered on the expected position of [C II] based on the redshift determined from the Mg II line ($\nu_{\text{obs}} = 252.496$ GHz). This tuning frequency is shown here as zero point of the velocity scale. The red solid curve is a fit to the data consisting of two Gaussians plus continuum. The [C II] line is detected at high significance and is redshifted by 566 ± 72 km s $^{-1}$ with respect to the Mg II redshift ($z_{[\text{C II}]} = 6.54122$, $z_{\text{Mg II}} = 6.527$). A second fainter line is observed at 254.45 ± 0.14 GHz. We find that the most likely identification for this line is a blended emission from the adjacent $3_{22} - 3_{13}$ and $5_{23} - 4_{32}$ H $_2$ O emission lines (see the text).

252.496 GHz, which corresponds to the expected [C II] frequency ($\nu_{\text{rest}} = 1900.539$ GHz) based on the quasar redshift estimated from the Mg II line: $z_{\text{Mg II}} = 6.527$ (Venemans et al. 2015). The observations were carried out on 2015 February 9 and 10 in the D configuration with a total time on source of only 3.55 hr (five antenna equivalent). The synthesized beam size is $2''.2 \times 1''.6$. The data were calibrated and analyzed with the IRAM GILDAS³ software package.

The final NOEMA spectrum of P036+03 is shown in Figure 1. Two lines are visible, a bright one, and a second fainter line on top of the underlying dust continuum. We fit two Gaussians plus continuum to the data and identify [C II] as the brightest of these lines. The [C II] line peaks at 252.02 ± 0.06 GHz, yielding a redshift of $z_{[\text{C II}]} = 6.54122 \pm 0.0018$ (i.e., redshifted by 566 ± 72 km s $^{-1}$ with respect to the Mg II redshift). The line has a FWHM = 360 ± 50 km s $^{-1}$ and a velocity integrated flux of 5.2 ± 0.6 Jy km s $^{-1}$. This corresponds to a [C II] luminosity of $L_{[\text{C II}]} = (5.8 \pm 0.7) \times 10^9 L_{\odot}$, which is a factor of ~ 1.4 brighter than the [C II] line in J1148+5251 ($4.2 \pm 0.4 \times 10^9 L_{\odot}$; Maiolino et al. 2005; Walter et al. 2009a). The second line peaks at 254.45 ± 0.14 GHz, i.e., blueshifted by -2863 ± 178 km s $^{-1}$ with respect to the [C II] line. This fainter line has a FWHM = 160 ± 100 km s $^{-1}$ and an integrated flux of 1.2 ± 0.7 Jy km s $^{-1}$. At our resolution, the most likely identification for this line is a blended water vapor emission from the adjacent $3_{22} - 3_{13}$ and $5_{23} - 4_{32}$ H $_2$ O transitions ($\nu_{\text{rest}} = 1919.359$ GHz and $\nu_{\text{rest}} = 1918.485$ GHz, respectively). This tentative blended water emission has a velocity

offset of 576 ± 165 km s $^{-1}$ with respect to its predicted value by the Mg II redshift. This offset is in good agreement with the velocity offset found for the [C II] line, reinforcing the identification of the water emission. Figure 2 shows the maps of the FIR continuum emission and the continuum subtracted [C II] emission.

Fitting the continuum flux density yields a value of 2.5 ± 0.5 mJy. We convert the measured dust continuum flux density to FIR luminosity, L_{FIR} , by modeling the FIR emission with an optically thin graybody spectrum and scale the model to match the observed dust continuum flux density. We use typical parameters in the model to reproduce the spectral energy distribution for high-redshift quasar host galaxies, i.e., a dust temperature of $T_d = 47$ K and a emissivity index of $\beta = 1.6$ (following, for example, Venemans et al. 2012; Willott et al. 2015). Integrating the model from rest-frame 42.5 to 122.5 μm we obtain the following L_{FIR} for P036+03: $L_{\text{FIR}} = (5.4 \pm 1.1) \times 10^{12} L_{\odot}$. Integrating the model from rest-frame 8 to 1000 μm we get a total infrared luminosity, L_{TIR} , of $L_{\text{TIR}} = (7.6 \pm 1.5) \times 10^{12} L_{\odot}$. We can use the total infrared luminosity to estimate the star formation rate using the relation $\text{SFR}_{\text{TIR}} (M_{\odot} \text{ yr}^{-1}) = \delta_{\text{MF}} \times 1.0 \times 10^{-10} L_{\text{TIR}} (L_{\odot})$ (Carilli & Walter 2013 and references therein), where δ_{MF} depends on the stellar population. We use $\delta_{\text{MF}} = 1.0$, which is appropriate for a Chabrier IMF. For P036+03, this relation results in $\text{SFR}_{\text{TIR}} = 760 \pm 150 M_{\odot} \text{ yr}^{-1}$. Alternatively, Sargsyan et al. (2014) show that even in sources dominated by active galactic nucleus (AGNs), the star formation rate can be estimated from $L_{[\text{C II}]}$ to a precision of $\sim 50\%$ with the relation $\text{SFR}_{[\text{C II}]} (M_{\odot} \text{ yr}^{-1}) = 10^{-7} L_{[\text{C II}]} (L_{\odot})$. This relation yields $\text{SFR}_{[\text{C II}]} = 580 \pm 70 M_{\odot} \text{ yr}^{-1}$, broadly consistent with the estimate above.

3. DISCUSSION

3.1. [C II]–IR Luminosity Relation

It has been shown that in local star-forming galaxies the ratio between the [C II] and IR luminosities is about 0.1%–1% but it decreases in galaxies with larger IR luminosities ($L_{\text{TIR}} > 10^{11} L_{\odot}$) such as LIRGs and ULIRGs. This has been known as the “[C II] deficit.” Similar deficits have been observed in other FIR lines such as [O I] 63.2 μm , [O I] 145 μm , and [N II] 122 μm . As a consequence, these trends are now being referred to as the “FIR lines deficit” (Graciá-Carpio et al. 2011). In Figure 3 we show the ratio of [C II] to TIR luminosity for different types of sources. The “[C II] deficit” can be clearly appreciated in the local samples: star-forming galaxies (Malhotra et al. 2001), LIRGs (Díaz-Santos et al. 2013), and ULIRGs (Luhman et al. 2003). The sample of IR-luminous star-forming galaxies, submillimeter galaxies, and quasars at $z > 1$ compiled by De Looze et al. (2014) and Brisbin et al. (2015) shows a larger scatter in the [C II] to TIR luminosity ratio ($\sim 10^{-4}$ – $10^{-1.5}$). The sample of $z \sim 6$ quasars with high IR luminosities studied by Maiolino et al. (2005), Walter et al. (2009), and Wang et al. (2013) shows small [C II] to FIR luminosity ratios, similar to what is observed in local ULIRGs ($\sim 10^{-3.5}$). One interpretation of such low ratios could be in part due to the central AGN contributing to the IR luminosity (Wang et al. 2013), but note that there is big literature dealing with possible explanations for the deficit (e.g., Malhotra et al. 2001; Graciá-Carpio et al. 2011; Díaz-

³ <http://www.iram.fr/IRAMFR/GILDAS>

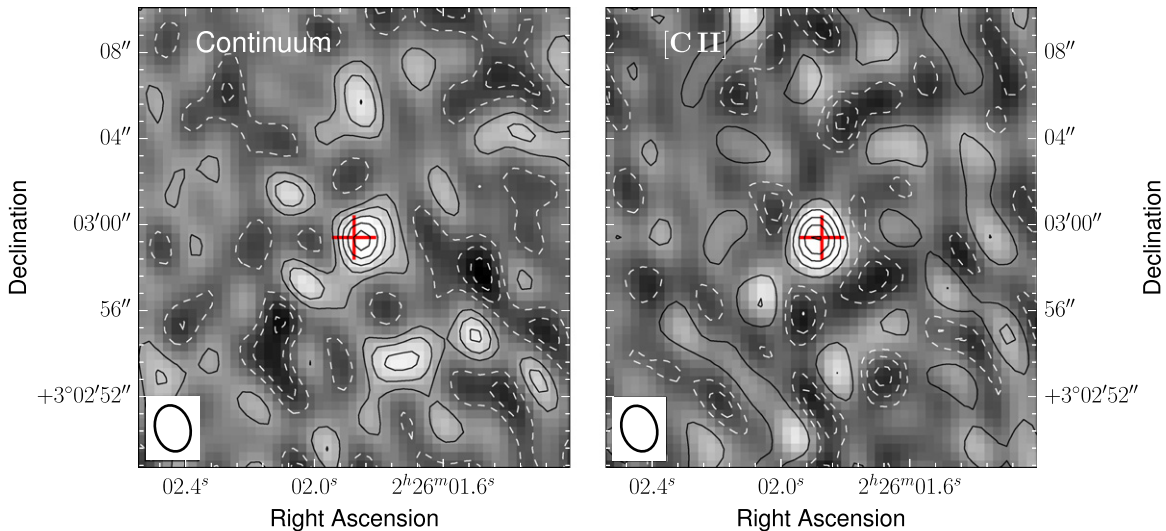


Figure 2. NOEMA cleaned maps of the $z = 6.5412$ quasar P036+03. The red cross in each panel shows the near-infrared location of the quasar. The beam size of $2''2 \times 1''6$ is shown at the bottom left of each panel. Left: far-infrared continuum emission obtained from line-free channels in the frequency range 254.274–252.524 GHz (i.e., 2100 km s⁻¹; see Figure 1). The contours correspond to -3σ , -2σ , -1σ (white dashed lines), 1σ , 2σ , 3σ , 4σ , and 5σ (black solid lines), with σ being the rms noise of 0.418 mJy beam⁻¹. Right: continuum subtracted [C II] emission integrated from the channels 251.372 to 251.782 GHz (i.e., 750 km s⁻¹). The contours are -3σ , -2σ , -1σ (white dashed lines), 1σ , 3σ , 5σ , 7σ , and 9σ (black solid lines), with $\sigma = 0.85$ mJy beam⁻¹. The excess of 3σ sources in the maps is due to the modest u , v coverage in our data.

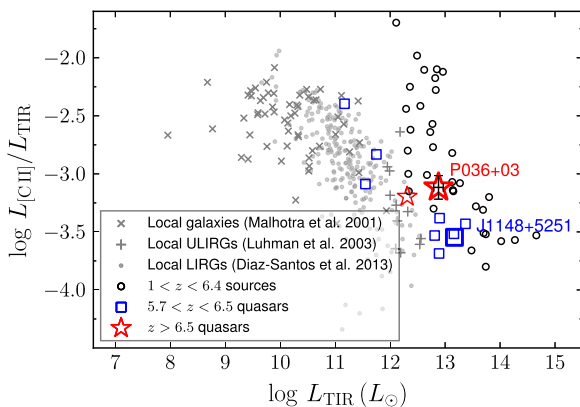


Figure 3. Ratio of [C II] to total IR luminosity (TIR; 8–1000 μ m) vs. TIR luminosity. The sources at $1.0 < z < 6.4$ include the compilation of star-forming galaxies, submillimeter galaxies, and quasars by De Looze et al. (2014) and eight star-forming galaxies recently reported by Brisbin et al. (2015). The $5.7 < z < 6.5$ quasars are from Bertoldi et al. (2003a), Maiolino et al. (2005), Walter et al. (2009a), Wang et al. (2013), Willott et al. (2013), and Willott et al. (2015). The $z > 6.5$ quasars are P036+03 (this work) and J1120+0641 at $z = 7.1$ (Venemans et al. 2012). Luminosities have been calculated with the cosmology used in this paper. The TIR luminosities for the $z > 5.7$ quasars have been consistently calculated as for P036+03 (see Section 2). The FIR (42.5–122.5 μ m) luminosities from Díaz-Santos et al. (2013) have been converted to TIR luminosities using a common conversion factor of 1.75 (Calzetti et al. 2000). Error bars are only plotted for P036+03 to enhance the clarity of the figure.

Santos et al. 2013). Willott et al. (2015) studied a sample of $z \sim 6$ quasars two orders of magnitudes fainter in the infrared ($L_{\text{TIR}} = 10^{11-12} L_{\odot}$). These quasars show ratios consistent with the local star-forming galaxies ($\sim 10^{-3} - 10^{-2.5}$). Venemans et al. (2012) report that the quasar J1120+0641 at $z = 7.1$ has a TIR luminosity that is between the Willott et al. (2015) sample and the IR-bright $z \sim 6$ quasars. The $L_{[\text{C II}]} / L_{\text{TIR}}$ ratio for J1120+0641 is more consistent with local star-forming galaxies than with ULIRGs. The quasar of the present study, P036+03, has an L_{TIR} comparable to other $z \sim 6$ quasars ($L_{\text{TIR}} \sim 10^{13}$

L_{\odot}). However, it has a significantly larger $L_{[\text{C II}]} / L_{\text{TIR}}$ ratio ($\sim 0.8 \times 10^{-3}$), similar to J1120+0641, and consistent with the lower end of local star-forming galaxies. This ratio is 2.7 times larger than the ratio reported for J1148+5251.

Together, this emphasizes the differences between the host galaxies of the most distant quasars. However, the number of quasars with [C II] and dust FIR continuum information is still too small to derive statistically meaningful trends or correlations.

3.2. Water Vapor Detection

The water vapor lines arise in the warm, dense phase of the ISM. They are one of the main coolants of this phase, thus playing a key role in the fragmentation and collapse of gas clouds (Carilli & Walter 2013). To date, there are only a handful of water vapor lines reported at high redshift, mostly in strongly magnified sources (e.g., van der Werf et al. 2011; Omont et al. 2013) and in one extreme submillimeter galaxy at $z = 6.3$ (Riechers 2013), which is the most distant detection of interstellar water to date. Recently, Bialy et al. (2015) showed that high abundances of water vapor could exist in galaxies with extremely low metallicity ($\sim 10^{-3}$ solar), as expected for the first generations of galaxies at high redshifts.

As discussed in Section 2, we identify a tentative detection of blended water vapor emission from the $3_{22} - 3_{13}$ and $5_{23} - 4_{32}$ H₂O transitions (see Figure 1). Owing to the low significance of the detection, it is difficult to make any strong conclusions, especially because the water emission is complex and hard to interpret if only one transition is measured (González-Alfonso et al. 2014). However, additional water transitions could be detectable in this source. For example, the $3_{21} - 3_{12}$ H₂O transition ($\nu_{\text{rest}} = 1162.912$ GHz) at $z = 6.5412$ is shifted into the 2 mm band and could simultaneously be observed with the CO($J = 10 \rightarrow 9$) line ($\nu_{\text{rest}} = 1151.985$ GHz). The detection of these transitions would lead to an improved excitation model for one of the earliest galaxies

known in the universe and to the confirmation of the most distant water detection to date.

4. SUMMARY

We detect a bright [C II] emission and the underlying continuum emission in P036+03, the most luminous quasar known so far at $z > 6.5$. A second line is tentatively detected, which we identify with blended water emission from the adjacent $3_{22} - 3_{13}$ and $5_{23} - 4_{32}$ H₂O transitions. If confirmed, this would be the highest-redshift detection of water vapor available to date.

The [C II] to TIR luminosity ratio in P036+03 is $\sim 0.8 \times 10^{-3}$, i.e., consistent with low- L_{TIR} star-forming galaxies and high compared to other IR-luminous quasars at $z > 6$. This ratio is a factor of ~ 3 higher than in J1148+5251 and consistent with the ratio in the most distant quasar known to date (Figure 3), emphasizing the diversity of quasar host galaxies in the early universe.

P036+03 rivals the current archetypal high-redshift quasar, J1148+5251 ($z = 6.42$), in both UV and [C II] luminosities. As a result of its brightness and given its convenient equatorial location, P036+03 can be studied from facilities in both hemispheres (in contrast to the northern source J1148+5251). For example, P036+03 would be an ideal target for high-resolution ALMA imaging to study the ISM physics and to search for signs of mergers, outflows, and feedback in one of the earliest galaxies in the universe. This quasar will thus likely become one of the key targets for studying star formation and the ISM in the early universe.

We are grateful to K. Schuster for the generous allocation of discretionary time. We thank J.M. Winters for his support in the implementation of this program. E.B. thanks C. Ferkinhoff for useful discussions. E.B. is a member of the IMPRS for Astronomy & Cosmic Physics at the University of Heidelberg, Germany. R.D. is supported by the DFG priority program 1573 “The physics of the interstellar medium.” B.P.V. and E.P.F. acknowledge funding through the ERC grant “Cosmic Dawn.”

Facility: IRAM:Interferometer.

REFERENCES

- Bertoldi, F., Carilli, C. L., Cox, P., et al. 2003a, *A&A*, 406, L55
 Bertoldi, F., Cox, P., Neri, R., et al. 2003b, *A&A*, 409, L47
 Bialy, S., Sternberg, A., & Loeb, A. 2015, *ApJ*, in press (arXiv:1503.03475)
 Brisbin, D., Ferkinhoff, C., Nikola, T., et al. 2015, *ApJ*, 799, 13
 Calzetti, D., Armus, L., Bohlin, R. C., et al. 2000, *ApJ*, 533, 682
 Carilli, C. L., & Walter, F. 2013, *ARA&A*, 51, 105
 Carnall, A. C., Shanks, T., Chehade, B., et al. 2015, *MNRAS*, submitted (arXiv:1502.07748)
 De Looze, I., Cormier, D., Lebouteiller, V., et al. 2014, *A&A*, 568, A62
 Díaz-Santos, T., Armus, L., Charmandaris, V., et al. 2013, *ApJ*, 774, 68
 Fan, X., Strauss, M. A., Schneider, D. P., et al. 2003, *AJ*, 125, 1649
 González-Alfonso, E., Fischer, J., Aalto, S., & Falstad, N. 2014, *A&A*, 567, A91
 González-López, J., Riechers, D. A., Decarli, R., et al. 2014, *ApJ*, 784, 99
 Graciá-Carpio, J., Sturm, E., Hailey-Dunsheath, S., et al. 2011, *ApJL*, 728, L7
 Kanekar, N., Wagg, J., Ram Chary, R., & Carilli, C. L. 2013, *ApJL*, 771, L20
 Luhman, M. L., Satyapal, S., Fischer, J., et al. 2003, *ApJ*, 594, 758
 Maiolino, R., Carniani, S., Fontana, A., et al. 2015, *MNRAS*, submitted (arXiv:1502.06634)
 Maiolino, R., Cox, P., Caselli, P., et al. 2005, *A&A*, 440, L51
 Maiolino, R., Gallerani, S., Neri, R., et al. 2012, *MNRAS*, 425, L66
 Malhotra, S., Kaufman, M. J., Hollenbach, D., et al. 2001, *ApJ*, 561, 766
 Omont, A., Yang, C., Cox, P., et al. 2013, *A&A*, 551, A115
 Ota, K., Walter, F., Ohta, K., et al. 2014, *ApJ*, 792, 34
 Ouchi, M., Ellis, R., Ono, Y., et al. 2013, *ApJ*, 778, 102
 Planck Collaboration, Ade, P. A. R., Aghanim, N., et al. 2014, *A&A*, 571, A16
 Riechers, D. A. 2013, *ApJL*, 765, L31
 Riechers, D. A., Walter, F., Bertoldi, F., et al. 2009, *ApJ*, 703, 1338
 Sargsyan, L., Samsonyan, A., Lebouteiller, V., et al. 2014, *ApJ*, 790, 15
 Schaerer, D., Boone, F., Zamojski, M., et al. 2015, *A&A*, 574, A19
 van der Werf, P. P., Berciano Alba, A., Spaans, M., et al. 2011, *ApJL*, 741, L38
 Venemans, B. P., Bañados, E., Decarli, R., et al. 2015, *ApJL*, 801, L11
 Venemans, B. P., McMahon, R. G., Walter, F., et al. 2012, *ApJL*, 751, L25
 Walter, F., Bertoldi, F., Carilli, C., et al. 2003, *Natur*, 424, 406
 Walter, F., Carilli, C., Bertoldi, F., et al. 2004, *ApJL*, 615, L17
 Walter, F., Decarli, R., Carilli, C., et al. 2012, *ApJ*, 752, 93
 Walter, F., Riechers, D., Cox, P., et al. 2009a, *Natur*, 457, 699
 Walter, F., Weiß, A., Riechers, D. A., et al. 2009b, *ApJL*, 691, L1
 Wang, R., Wagg, J., Carilli, C. L., et al. 2013, *ApJ*, 773, 44
 Watson, D., Christensen, L., Knudsen, K. K., et al. 2015, *Natur*, 519, 327
 Willott, C. J., Bergeron, J., & Omont, A. 2015, *ApJ*, 801, 123
 Willott, C. J., Omont, A., & Bergeron, J. 2013, *ApJ*, 770, 13
 Wu, X.-B., Wang, F., Fan, X., et al. 2015, *Natur*, 518, 512